A Perturbation Method for Hurricane Ensemble Predictions

Z. ZHANG AND T. N. KRISHNAMURTI

Department of Meteorology, The Florida State University, Tallahassee, Florida

(Manuscript received 3 October 1997, in final form 13 April 1998)

ABSTRACT

This study illustrates the capability of the ensemble technique to improve hurricane forecasts in the Florida State University Global Spectral Model. A perturbation method for hurricane ensemble prediction is proposed. The perturbation method consists of perturbing hurricane initial position and the large-scale environment in which the storm is embedded. The position perturbation is done by displacing the observed hurricane toward different directions by a small distance. The empirical orthogonal function (EOF) analysis is used to find fast-growing modes in the initial state. It is shown that the model forecasts, in terms of both hurricane track and other physical variables, are very sensitive to the hurricane initial position, intensity, and its large-scale environment. The results also show the EOF-based perturbations are the fast-growing modes and can be used to reduce the initial uncertainty in the analysis.

The hurricane forecast obtained from ensemble statistics lead to a large improvement in the track forecasts. For the intensity forecasts, the ensemble prediction provides several statistical methods to display the forecasts. The statistical mean from individual ensemble members provide an overview of the forecast. The spatial distribution of the probability of predicted variables make it possible to find the most likely weather pattern.

1. Introduction

It has long been recognized that there are two main sources of forecast errors in numerical weather prediction (NWP) models: the deficiencies in the numerical models and the imperfect knowledge of the initial state of the atmosphere. The former arises from the discrepancy between a numerical model and the real atmosphere—that is, the model approximation to the real atmospheric dynamics and physics. The latter is due to the fact that the initial state of the real atmosphere will never be observed accurately enough because of the instrumentation error and the low resolution of the observational network. Over the last three decades, due to use of supercomputers and a better understanding of atmospheric physics, the improved model dynamics and physics have contributed to a major improvement of the model forecast skill. Thus, the forecast errors due to the growth of external error have been significantly reduced (Krishnamurti and Bedi 1988; Krishnamurti et al. 1983). On the other hand, less attention has been paid to the forecast errors due to inaccurate initial observations until recently. The first works that addressed the importance of initial states to forecast errors were made by Lorenz (1963, 1965). In his pioneering works, Lorenz pointed out that in some deterministic nonlinear dynamical systems, slightly different initial states may lead to considerably different final solutions. The atmosphere is a prime example of this kind of dynamical system. Since one cannot avoid observational errors in the initial analysis, these initial errors will grow with integration time through a self-applied mechanism. Therefore, model forecast skill will decrease with increasing forecast length even if the model itself is perfect. To some extent, the atmospheric system should be treated as a statistical system rather than as a deterministic system.

The stochastic dynamical system, introduced by Epstein (1969), can predict not only the conventional prognostic variables but also their statistics, such as expectation and variance. The main problem of this approach is that it requires a large amount of computer resources as well as a physical-based closure scheme.

Ensemble prediction takes a different approach to achieve the same goal. The basic idea of an ensemble forecast is that since the true state of the atmosphere at any time can be only approximately observed, a statistical mean of a set of model forecasts, starting from slightly different initial states, might help to reduce the impact of the initial data uncertainties on the final forecast. Therefore, the key to a successful ensemble forecast lies in how one generates a set of initial states that is slightly different from the original analysis and represents real initial model uncertainty. This problem has recently attracted much attention.

Random error is the main source of observation error. It is reasonable to assume that the initial errors around the true atmospheric state are randomly distributed. This is the basic idea of the Monte Carlo method. The Monte

Corresponding author address: Dr. Zhan Zhang, Department of Meteorology, The Florida State University, Tallahassee, FL 32306.

Carlo method was first applied to a numerical model by Leith (1974) in a perfect model environment. He demonstrated that Monte Carlo prediction resulted in a practical approximation to the stochastic dynamical technique (Epstein 1969) and the ensemble mean provides a more skillful forecast than the control run—that is, the forecast that starts from the best estimated initial state. Obviously, the success of the Monte Carlo forecasting scheme depends upon the sample size. It is apparent that the Monte Carlo method is not an efficient way to generate initial perturbations. The reasons are the following: first, in order to sample all of the possibilities of the initial state, a very large number of samples is needed, which is not feasible for an operational global spectral model with higher resolution. Second, research indicates (Toth and Kalnay 1993, 1998) the errors in the analysis are no longer random. During the course of model integration in the analysis cycle, some error modes are suppressed while others grow rapidly with time. In other words, the model has an inherent tendency to select those modes that grow the fastest. This preference depends upon the basic state of the atmosphere. The consequence of this selection rule is that the analysis error fields will be dominated by fast-growing modes. Therefore, the perturbations that will contribute to the final ensemble forecast should be those that have components projected onto the growing modes. It has been well recognized (Palmer et al. 1992; Toth and Kalnay 1993) that the optimal perturbations for an ensemble forecast are the fast-growing modes. Use of the fast-growing modes as initial ensemble perturbations can significantly reduce the number of samples. Several perturbation methods have been developed based on this idea (Hoffman and Kalnay 1983; Ebisuzaki and Kalnay 1991). Two commonly used methods were implemented in both the U.S. National Centers for Environmental Prediction (NCEP) and European Centre for Medium-Range Weather Forecasts (ECMWF) operational ensemble forecasting systems in December 1993. Although the methods used in the NCEP and the ECMWF systems to generate ensemble perturbations are somewhat different, NCEP uses ''breeding'' vector method (Toth and Kalnay 1993) while ECMWF uses singular vector method (Palmer et al. 1992), they are based on the same idea—that is, fast-growing modes are the optimal perturbations for ensemble prediction. Many research works are based on these two methods (Buizza 1997; Hamill and Colucci 1997; Houtekamer and Lefaivre 1997; Tracton and Kalnay 1993).

One should note that most of the research works mentioned above have concentrated on midlatitude weather systems. Less emphasis has been placed on the ensemble prediction techniques for the tropical weather systems. It is necessary to develop an adequate perturbation method for hurricane ensemble prediction. Since the dynamics and physics in the tropical atmosphere are quite different from those in the midlatitudes, the methods for the perturbation generation successfully used in midlatitudes are not necessarily the most adequate for the tropical environment. It is well known that the perturbation growth over midlatitudes is mainly a consequence of dynamical instability according to linear perturbation theory. However, the perturbation growth mechanism is quite different in the Tropics. Although it is still not clear, some physical processes, such as cumulus convection and latent heating together with their interactions with large-scale (synoptic-scale) dynamics, might be the more important factors responsible for the perturbation growth over the Tropics. This necessitates the inclusion of full model physics in the procedure for generating optimal perturbations over the Tropics.

The purpose of this study may be summarized as follows.

- Study the general properties of the optimal perturbations over the tropical regions arising from slightly different initial states. In this study, one assumes that the real atmosphere is accurately represented by model dynamics and physics.
- Develop an alternative method to generate optimal initial perturbations for use in ensemble forecasting over the tropical domain. A complex EOF analysis technique will be utilized in this proposed method.
- Examine the proposed method by performing several hurricane case studies to see if there is any improvement in hurricane predictions.

The methodology is presented in section 2. A perturbation method for hurricane ensemble predictions is proposed and described in detail, which includes hurricane position and its environment perturbations. Section 3 presents a brief description of the Florida State University (FSU) Global Spectral Model, which is used in this study. Experimental design strategies are discussed in section 4. This section also explains how and why the various hurricane cases were chosen. The results from all of the experiments are presented in section 5 and they include: the general properties of EOF-based perturbations, the comparison among ensemble predictions, control and observed track, and the comparison of predicted model variables between ensemble and control experiments.

2. Methodology

It is commonly accepted that there are three factors in the initial state of an NWP model that may affect the accuracy of a hurricane forecast: (a) large-scale environmental steering flows, (b) intensity of the hurricane, (c) and the observational accuracy of the hurricane position. Removing or reducing the uncertainty of any of these three factors at the initial state will, most likely, lead to an improvement in hurricane prediction. Therefore, the procedure for generating initial ensemble perturbations should invoke these factors. In other words, both initial position and large-scale environmental per-

TABLE 1. Hurricane position errors in different observations.

Observational means	Aircraft reconnaissance	Radar	Satellite imagery
Position errors (km)	~20	20 ~ 55	~110

turbations are important to the hurricane ensemble prediction. In the next two sections, we shall discuss a perturbation method that may be suitable for hurricane ensemble prediction.

a. Position perturbation

Table 1 shows typical observational errors for initial hurricane position from different means. It is apparent that observed location of hurricane could be in error by ~50 km. Many researchers have demonstrated that the accuracy of a hurricane position at the initial state is crucial to the numerical model track forecast (Kurihara et al. 1993; Ross and Kurihara 1992; Radford and Chan 1995). To incorporate the uncertainty of hurricane positions in its initial state, one must perturb the analyzed position by displacing its location by 50 km to the north, south, east, and west (Fig. 1). Thus, by perturbing the initial hurricane positions, one generates five ensemble initial states. This is the simplest way to perturb the hurricane position. It implies a homogeneous hurricane position error distribution; that is, the initial position errors have no preference for any particular direction. Also, it is difficult to determine the initial position error preference from ECMWF analysis because it is prepared for medium-range large-scale prediction, which usually carries less or no information about hurricane position.

b. EOF-based perturbation

The field perturbation method proposed here is based on the fact that during the first few days of the model integration the perturbation grows linearly. Figure 2 shows a schematic of this method. The procedures of this method may be described as follows:

- add random perturbations with magnitudes that are comparable to the forecast errors of the control analysis;
- integrate the model with its full physics for 36 h, starting from the unperturbed (control) as well as the perturbed initial states. The output of the forecast results are stored for every 3 h;
- subtract the control forecast from the perturbed forecast at corresponding times to obtain the time series of difference field forecasts;
- perform an EOF analysis for the time series of the difference fields over the region of interest. Those modes (eigenvectors) whose EOF coefficients increase rapidly with time are considered as the fast-growing modes, and thus, can be used as initial perturbations for the ensemble prediction;
- an ensemble of initial states is generated by adding/subtracting these EOF-based perturbations to/from the control analysis.

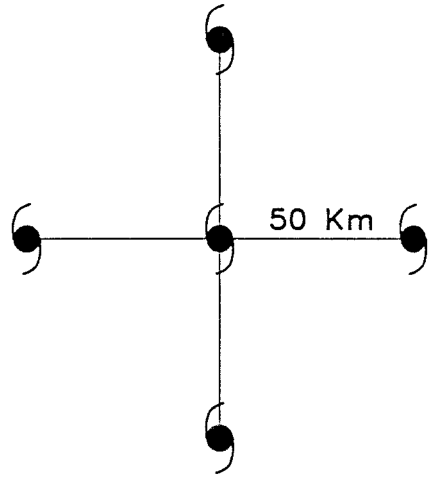

FIG. 1. Schematic diagram of hurricane initial position.

This method is called ‘‘EOF-based perturbation method.’’ Since the EOF-based perturbation is calculated over the period of 0–36 h but applied to the initial time, it is assumed that the basic flow evolves slowly. It is particularly true for the tropical environment. Since the interest of this study lies in the impact of ensemble prediction on tropical weather systems, such as a hurricane, we shall apply this method over the Tropics. It

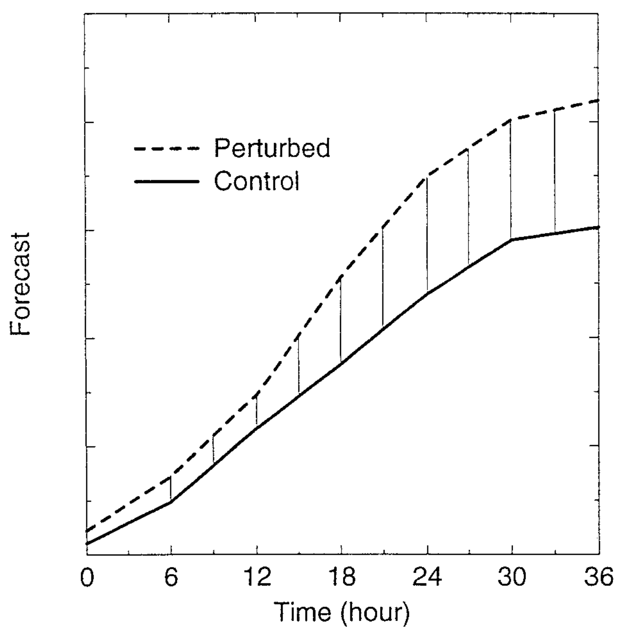

FIG. 2. Schematic diagram of the generation of an EOF-based perturbation.

is generally agreed that unlike midlatitude disturbances, the wind field is more important, for large-scale flows, than geopotential height field in the Tropics. To reduce the computational requirements, only the wind and the temperature fields will be subjected to an EOF analysis. Temperature analysis will be performed using scaler EOF analysis, whereas a complex EOF analysis technique will be utilized to handle the wind field, because it permits the depiction of phase changes (Legler 1983). Also, only the EOF eigenmode corresponding to largest eigenvalue will be used in this study. If one applies this method to each of five ensemble members generated from position perturbations, one will have three members for each position—that is, original, original plus, and minus EOF-based perturbation. A total of 15 ensemble members are generated based on the perturbations of the positions and fields.

Another issue that must be dealt with is the magnitude of the perturbations. As discussed before, the fast-growing modes will dominate in the initial field, no matter how small their initial magnitudes are. This is because it is the pattern not the magnitude that determines the growth rate of these modes. In other words, even a decaying mode can have a large magnitude at the initial state. However, it will be suppressed during the course of model integration and become considerably reduced in magnitude. It is reasonable to assume that the perturbations have an order of magnitude comparable to that of 3-h forecast error, which is around 3 m s^{-1} for the wind field and 0.6 K for the temperature field.

Now, we will describe the mathematics of the EOF perturbation method. Let δu and δv be the components (δu positive to the east, δv positive to the north) of the difference wind fields—that is, the difference between the perturbed forecast and the control forecast at 3-h intervals). Then a complex vector at each Gaussian grid point can be written by combining δu and δv:

$$\delta w_{s,t} = \delta u_{s,t} + i\delta v_{s,t}, \qquad (1)$$

where δu and δv are defined as:

$$\delta u_{s,t} = u^p_{s,t} - u^c_{s,t} \qquad (2)$$

$$\delta v_{s,t} = v^p_{s,t} - v^c_{s,t}. \qquad (3)$$

Superscript p and c indicate ‘‘perturbed’’ and ‘‘control’’ run, and subscript s and t represent the indices of space and time, respectively.

The entire dataset then can be expressed as $T \times S$ rectangular matrix:

$$\mathbf{W} = \begin{pmatrix} \delta w_{11} & \delta w_{12} & \cdots & \delta w_{1S} \\ \delta w_{21} & \delta w_{22} & \cdots & \delta w_{2S} \\ \cdots & \cdots & \cdots & \cdots \\ \delta w_{T1} & \delta w_{T2} & \cdots & \delta w_{TS} \end{pmatrix}. \qquad (4)$$

The covariance matrix is defined as:

$$\mathbf{H} = \frac{1}{T}\mathbf{W}^*\mathbf{W}, \qquad (5)$$

where $\mathbf{W}^*$ denotes the complex conjugate transpose of $\mathbf{W}$. Obviously, $\mathbf{H}$ is a Hermitian matrix and by definition,

$$\mathbf{H} = \mathbf{H}^*, \qquad (6)$$

$\mathbf{H}$ is symmetric and is composed of complex elements, except for the diagonals, which are real. The diagonal elements are proportional to the perturbation kinetic energy for each grid point.

Suppose $\mathbf{e}_i$ and λ_i are eigenvectors and eigenvalues of matrix $\mathbf{H}$, and eigenvectors $\mathbf{e}_i$ are in descending order according to the magnitude of eigenvalues λ_i. Then the dataset matrix $\mathbf{W}$ can be expanded with respect to the base of eigenvectors $\mathbf{e}_i$:

$$\mathbf{W} = \mathbf{YE}, \qquad (7)$$

where matrix $\mathbf{E}$ consists of row vectors of $\mathbf{e}_i$, which are a function of space only, normally defined as the EOF. Matrix $\mathbf{Y}$ contains coefficients for different eigenvectors at different times and is a function of time only. Here, $\mathbf{Y}$ is called the principal component (PC). The fast growing modes are easily selected by looking at the time evolution of the EOF coefficients. Those modes whose coefficients increase rapidly with time will be denoted as the fast-growing modes and are selected.

The CPU time of this method is comparable with that of NCEP breeding method. For each perturbed hurricane position, only one pair of model integrations, starting from control and randomly perturbed analysis, is needed to generate EOF-based perturbations. Therefore, this method is feasible for operational hurricane prediction.

3. FSU global spectral model

The NWP model used in this study is the FSU Global Spectral Model and has been described in Krishnamurti et al. (1989) and Zhang (1997). The model has a very good forecast skill, especially for tropical weather systems, such as a hurricane, the summer monsoon, etc.

The physical processes in the NWP model are very important, especially for the tropical region. Generally speaking, the fast-growing modes in the Tropics are mainly determined by model physics. The complete model physics include

- fourth-order horizontal diffusion;
- Kuo-type cumulus parameterization;
- shallow convective adjustment;
- dry convective adjustment;
- large-scale condensation;
- surface fluxes by means of a similarity theory, parameterization of planetary boundary layer;
- vertical distribution of fluxes using diffusive functions of the Richardson number;
- longwave and shortwave radiative fluxes based on a band model;
- diurnal solar cycle;
- parameterization of low, middle, and high clouds based on threshold relative humidity for radiative transfer calculations;

TABLE 2. Hurricane experiments.

Hurricane	Initial position lat–long	Model initial date* and time (UTC)	Initial intensity pressure (hPa)	Track type
Gilbert	16.1°N, 69.5°W	880911 1200	975	Westward
Hugo	12.5°N, 34.8°W	890912 1200	998	Westward
Andrew	25.3°N, 65.9°W	920822 1200	1000	Westward
Florence	27.3°N, 53.4°W	941104 1200	999	Recurved
Opal	21.0°N, 92.3°W	951002 1200	973	Recurved

* yymmdd where: yy are the last two digits of the year, mm is the month of the year, and dd is the day of the month.

- surface energy balance coupled to the similarity theory; and
- envelope orography.

4. Experiment design

The main concerns of this study are to apply the ensemble technique to hurricane prediction using a numerical model, and to investigate the patterns of the fast-growing modes in the Tropics, that is, possible realistic perturbations generated by the numerical model in the hurricane environment. To achieve these purposes, the experiments need to be carefully designed.

There have not been many published papers in the literature that address the subject of hurricane ensemble prediction. This is mainly because a theory for the generation of ensemble perturbations for the tropical regions has been lacking. As mentioned in the introduction, the current ensemble prediction theories were developed mainly for midlatitude weather systems and it was necessary to develop a perturbation theory for tropical ensemble prediction.

Krishnamurti et al. (1997) attempted to apply an ensemble forecast technique to hurricane track prediction using a numerical model. They used a single multilevel global spectral model that starts model integrations from the same start date, but from the initial states analyzed by various modeling centers. They carried out the track forecasts from different analysis for 5 days. The main finding of their study was that the spread of an ensemble of hurricane forecast tracks was drastically reduced as a result of using physical initialization, as compared to control runs, which did not use rain-rate initialization.

The following problems should be taken into account in the design of the experiments:

1) the features of efficient perturbations for the hurricane prediction;
2) the impact of ensemble technique on hurricane prediction;
3) the sensitivity of hurricane track forecast to its initial position [only brief discussions will be given. Details of results are provided in a separate paper (Zhang and Krishnamurti 1997)]; and
4) the sensitivity of hurricane fields forecast to its initial intensity and environmental analysis.

The hurricane cases, chosen here, were based on the concerns discussed above. Table 2 summarizes the main features of the hurricane experiments of this study. All of the cases chosen occurred over the Atlantic Ocean. Some of them had straight westward moving tracks, whereas others exhibited a recurvature. For each case, we ran one control experiment, whose integration begins from a conventional analysis; this was followed by a 15-member ensemble forecast. The generation of the ensemble members has been discussed in the previous section.

5. Results

Here we shall mainly discuss the performance of the proposed method for Hurricane Gilbert of 1988.

a. EOF-based perturbations

Figure 3 shows an example of the normalized EOF coefficients corresponding to different EOF eigenmodes of the wind perturbations varying with time. It is apparent that the EOF coefficients corresponding to the largest eigenvalue have an increasing tendency with respect to time. Other coefficients either oscillate or decay with time. It should be noted that the initial amplitudes of the EOF coefficients corresponding to largest eigenvalues are not always greater than the amplitudes of other coefficients. For example, in Fig. 3, the initial amplitude of the coefficient with largest eigenvalue has the smallest amplitude compared to the other coefficients at the initial time. It is clear that growth rate, rather than the initial amplitude, is more important for the ensemble perturbations.

Therefore, those EOF eigenmodes whose coefficients increase rapidly with time could be the fast-growing modes under certain initial conditions. It is possible that these eigenmodes could be the fast-growing modes for the initial basic state.

Figures 4–5 are the wind perturbations, corresponding to the largest EOF added to the initial state and their evolutions in time for the Hurricane Florence case, at 1000 hPa and 500 hPa, respectively. The top panel corresponds to the perturbation fields at hour 0, and the bottom panel represents hour 36. By analyzing the perturbations obtained from all of the experiments, we

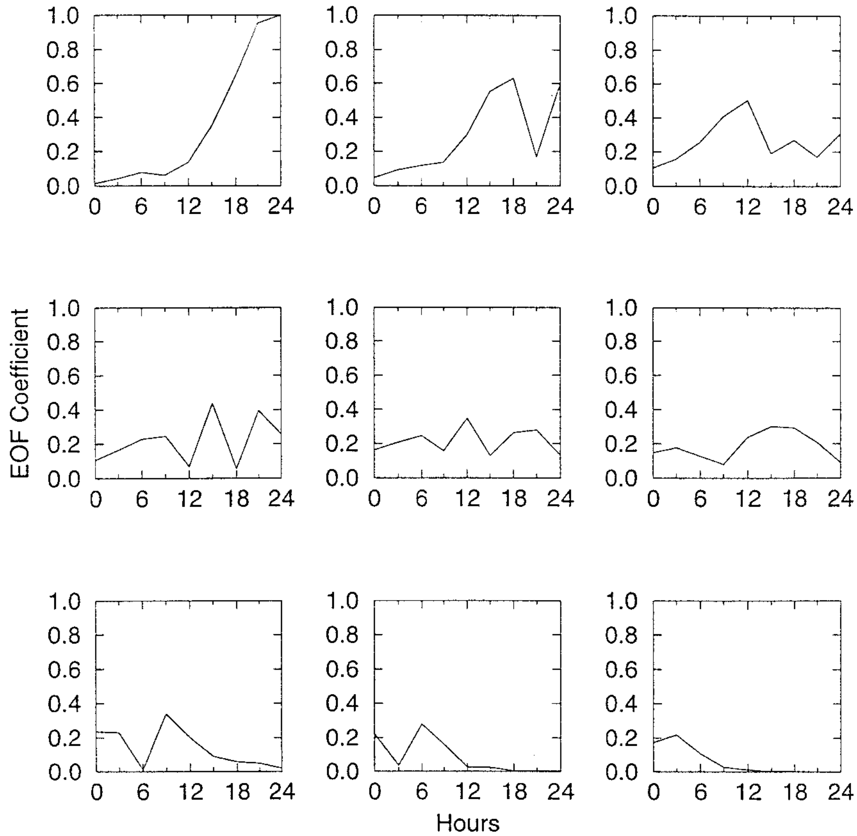

FIG. 3. Hurricane Gilbert: EOF coefficients (amplitude) of wind field for different eigenmodes. Corresponding to first to ninth eigenmodes from top left to bottom right.

found that the following features were common to the EOF-based perturbation fields.

1) Although the initial perturbations are randomly distributed, the EOF perturbation patterns are well organized.
2) The magnitudes of the perturbations are area dependent. The maximum amplitude occurs over regions where there are strong weather systems, such as in the vicinity of the hurricane. Over other regions, the value of the perturbations were relatively small.
3) The structure of the perturbations were quite different from those of the midlatitudes where baroclinic-instability-related features dominated the perturbation field. The barotropic structures can be clearly seen in the wind perturbation fields at hour 0. For instance, there is a perturbation center at 1000 hPa in wind perturbation field (Fig. 4), which is also present at the same location at 500 hPa (Fig. 5).

For comparison, random perturbation of the 1000 hPa wind fields at hour 0 (Fig. 6 top) and hour 36 (Fig. 6 bottom) for the same case are shown. It is apparent that the growth rate of the random perturbations are much smaller that those of the EOF-based perturbations. The random perturbations at hour 36 remained nearly the same magnitude as those of the initial perturbations. However, the EOF-based perturbations grew very rapidly. The initial amplitude of the EOF-based wind perturbations was only 3 m s^{-1}; however, the maximum perturbations for the wind field at hour 36 reached a magnitude of 12 m s^{-1}.

It should be noticed that, because the EOF-based perturbations are computed from a time average of the spatial covariance of the evolving perturbation at 3-h intervals, they actually represent the average growing modes over the period of 0–36 h. Since a growing mode tends to grow fast, especially around hurricanes, the EOF perturbations are dominated by the latter stage of the growing modes. Therefore, if the EOF perturbations are applied to the initial time, the growth rate would be less than what shows in Fig. 3. The experiments in this study indicate that the EOF perturbation is still a good approximation to the growing mode for the basic flow at initial time.

b. Track predictions

The results of track predictions have been discussed in a separate paper by Zhang and Krishnamurti (1997). We will only briefly summarize the results here.

Figure 7 is an example of the ensemble track forecast product. It shows the comparison of track forecasts for

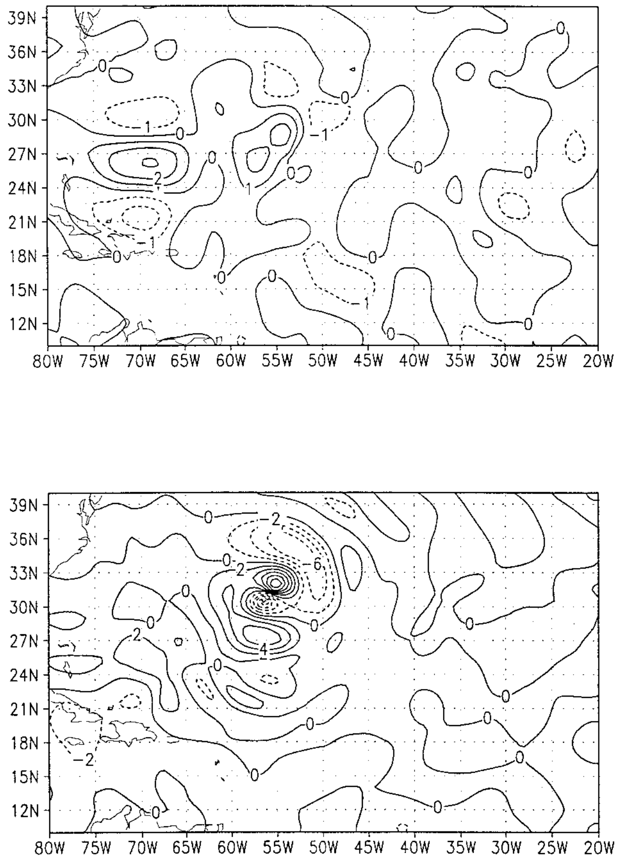

FIG. 4. Hurricane Florence: EOF-based wind perturbations at 1000 hPa (top) at hour 0 and (bottom) at hour 36. The contour is isotach of wind speed.

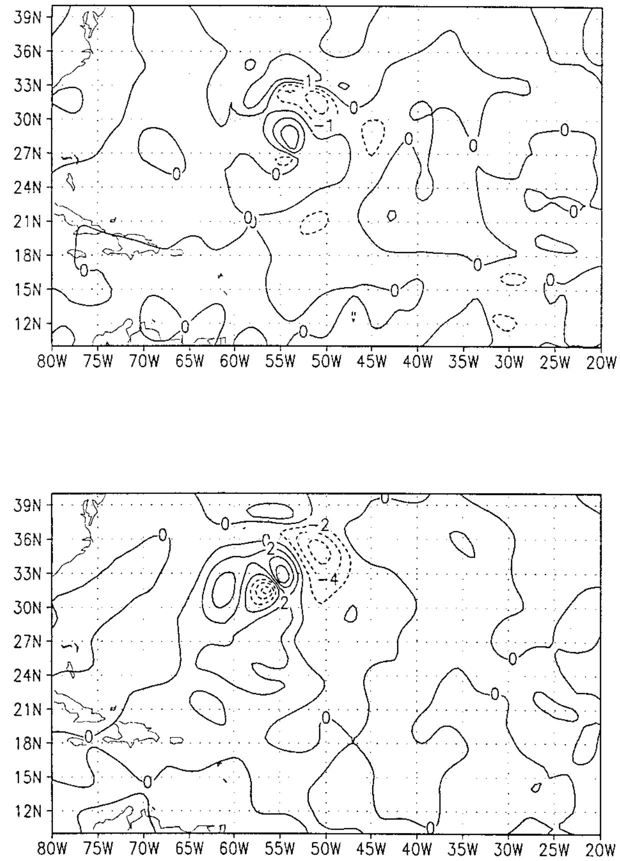

FIG. 5. Hurricane Florence: EOF-based wind perturbations at 500 hPa (top) at hour 0 and (bottom) at hour 36. The contour is isotach of wind speed.

Hurricane Gilbert between ensemble and control experiments. The model forecast starts from 1200 UTC 11 September 1988.

Three ensemble-averaged tracks were calculated to represent ensemble track predictions in Fig. 7. Here the full ensemble mean represents the average track forecast over all of the ensemble members. The selected ensemble mean is an average over those ensemble members whose 12-h predicted hurricane positions are close enough to the observed hurricane position at that time. This assumes that by the time the forecast is completed, the observed position at hour 12 of the forecast is available to us. A cluster analysis is also performed over all of the ensemble members in order to obtain a better idea of the direction of the hurricane track that a majority of the ensemble members would take. The cluster mean shown in Fig. 7 is based on a cluster that includes roughly 90% of the members of the ensemble.

It is clear that within the first 12 h of the forecast, the predicted hurricane positions from different ensemble members were very close to each other. The track spread starts at hour 12 of the forecast when most of the tracks were moving due west while a few exhibited deflection to the northwest. Comparison shows clearly that all of the ensemble-averaged tracks have smaller position errors than the track from the control experiment. The other feature that can be seen from Fig. 7 is that the hurricane positions from different ensemble members were scattered over a very large area on day 4 of the forecast, indicating the model track forecasts are indeed quite sensitive to the initial state.

c. *Predictions of wind fields and maximum wind probabilities*

From a practical point of view, the wind field forecast is a very important component in hurricane prediction, since stronger winds bring a higher risk of loss of life and property. Therefore, an accurate prediction of the location of maximum winds is critical for the decision makers. Unlike a single deterministic model forecast, an ensemble forecast model provides not only the wind intensity forecast, but also the probability of maximum winds striking a particular location.

In each grid point of the forecast domain, we have 15 forecasts from different ensemble members, including the control experiment. Therefore, a two-dimensional distribution of the probability that winds above

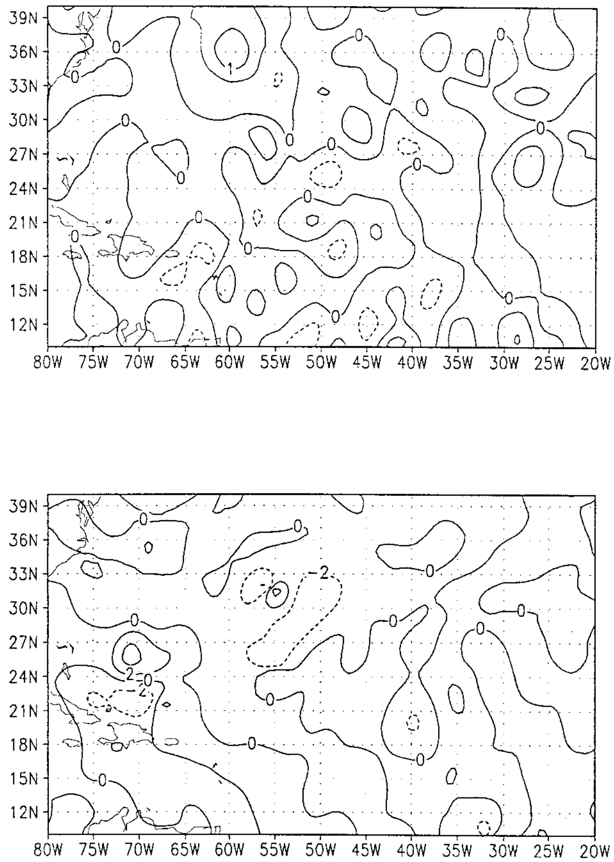

FIG. 6. Hurricane Florence: Random wind perturbations at 1000 hPa (top) at hour 0 and (bottom) at hour 36. The contour is the isotach of wind speed.

a certain speed will exist can be calculated for each grid point. In this study, it is assumed that each ensemble member is equally likely in the calculation of probabilities, and the probability is expressed as percentages of the maximum possible value; that is,

$$P_{\mathbf{X}}\{x_L < \mathbf{X} < x_U\} = \frac{N_{\text{sample}}}{N_{\text{total}}}, \tag{8}$$

where subscript **X** denotes any physical variable, and x_L and x_U are lower and upper limits of the physical variable **X**, respectively. Therefore, $P_{\mathbf{X}}$ gives the probability of any physical variable **X** whose value is within the range (x_L, x_U). Here, N_{sample} is the number of ensemble forecasts within the (x_L, x_U) range, and N_{total} is the number of total ensemble members (equal to 15 in this study). It should be noted that generally speaking, the control experiment should be given higher weight than any other ensemble members.

Figure 8 illustrates the 850-hPa wind field forecasts at hour 48 for the Hurricane Gilbert case. The top panel shows the streamlines and isotachs from the control experiment. The bottom panel is the streamlines from the ensemble mean prediction along with the probability of having wind speeds greater than 25 m s^{-1}. It appears that the location of the maximum wind speed of the control experiment is not coincident with the maximum probability of wind speed greater than 25 m s^{-1}. This disagreement between the maximum wind speed location from control experiment and the maximum probability of wind speed indicates that although the control experiment shows the maximum wind occurs in the northeast quadrant of the hurricane, most of the other ensemble forecasts predicted that strongest wind speeds occur to the north of the hurricane. It should also be noted that the predicted hurricane center from the ensemble experiment is located to the south of the control hurricane center, which is closer to the observed position. The hurricane in the control experiment is a relatively larger storm, and the streamlines are distorted by an unrealistic northeast to southwest weak band of wind speed extending from the hurricane center. The probability of wind speeds greater than 25 m s^{-1} exhibits a nice spatial distribution around the hurricane center.

The wind fields and their probability distributions for the Hurricane Andrew case were also calculated and are shown in Fig. 9. Figure 9 shows the 850-hPa streamlines and isotachs at forecast hour 48 and the corresponding spatial distribution of probability of wind speed greater than 25 m s^{-1} for Hurricane Andrew. The centers of strong wind speed and maximum probability are almost at the same location, but the probability center is extended to the west. The maximum probability of wind speed greater than 25 m s^{-1} is 87%.

The probability information is very useful. It not only can provide the likely maximum wind speed area (if not coincident with the wind forecast from control experiment) but also can help the forecaster to accurately locate the future hurricane positions. For instance, a forecaster can examine the steering flows provided by different ensemble members and find out what kind of large-scale steering flow will most likely guide the hurricane track. Sometimes, this work can be done by just looking at all of the information from the ensemble forecasts. In most of the cases, it was necessary to calculate the spatial distribution of the probability of the wind speed or even wind direction to obtain the most likely large-scale steering flows.

d. Surface pressure and wind speed at fixed locations

To take advantage of the products from ensemble forecasting, Molteni et al. (1996) suggested using a plot that shows time-evolving probabilities of forecast variables within specific ranges at a particular location to assess the ensemble dispersion. They referred to this kind of plot as ''plumes.'' The plumes are useful to the local forecasters only if we have large enough samples in our ensemble forecast. Otherwise, the calculated probability is not very beneficial due to the lack of samples.

On the other hand, it is felt that for hurricane pre-

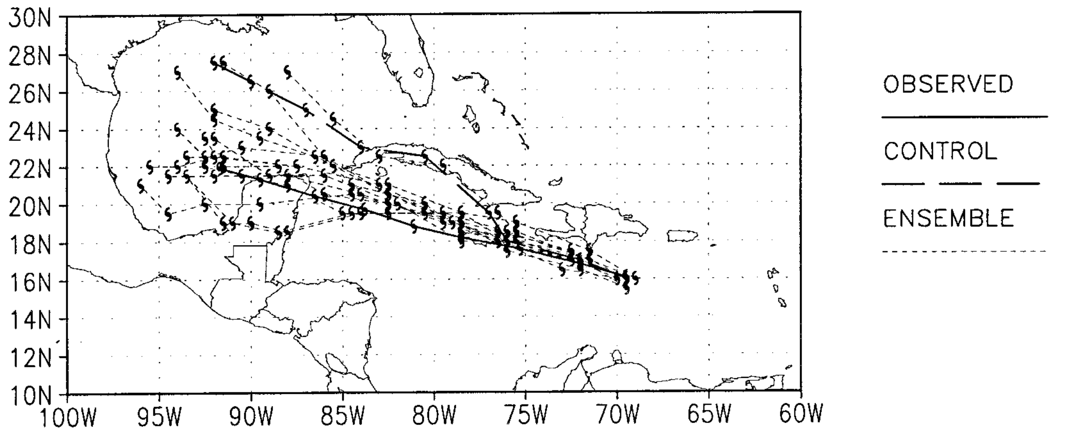

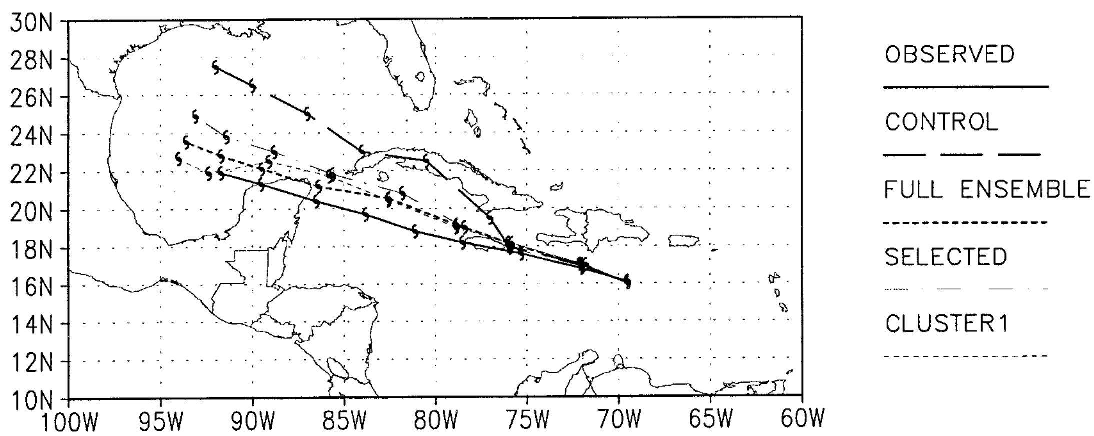

FIG. 7. Hurricane Gilbert track prediction, starting from 1200 UTC 11 Sep 1988. (top) The best track (solid line), the track from the control experiment, (long-dash line), and the track forecasts from different ensemble members (short-dash line). (bottom) The best track (solid line) compared with the full ensemble mean (heavier short-dash line), cluster 1 mean (short-dash line), track prediction from the control experiment (long-dash line), and selected track mean (lighter short-dash line).

diction, we are mostly concerned with the possible extreme values that could occur at a fixed location, whereas the probabilities for a single location may not be of interest. A time evolution of the forecast variable with maximum and minimum possible ranges would provide a better guidance to the local forecasters.

An approaching hurricane is characterized by a rapid increase in wind speed and decrease in surface pressure. Therefore, the time evolution of surface pressure and wind speed at a specific location along the path of the hurricane can be used to examine the performance of the forecast.

Figures 10–12 illustrate the forecasts of wind speeds and surface pressures from the control and the ensemble experiment at locations along the path of Hurricane Gilbert. The vertical bars indicate the range of the forecasts from different ensemble members. The dashed line is the line that links the middle point of the the maximum and minimum values. This line can be considered an ensemble forecast at this specific location. The selected locations are A (19.0°N, 78.5°W), B (18.0°N, 78.5°W). They are on or near to the observed track of Hurricane Gilbert. The center of Hurricane Gilbert passed locations A and B at approximately forecast hour 36. At locations A and B, the control and ensemble experiments reached their peak values of wind speed at hour 24, which indicates the hurricane is approaching the stations. The peak wind speed is about 28 m s^{-1} at station A and 31 m s^{-1} at station B for the control experiment. The ensemble peak wind speed is much stronger than that from the control experiment. Specifically, wind speed peaks at 35 m s^{-1} at station A and at about 40 m s^{-1} at station

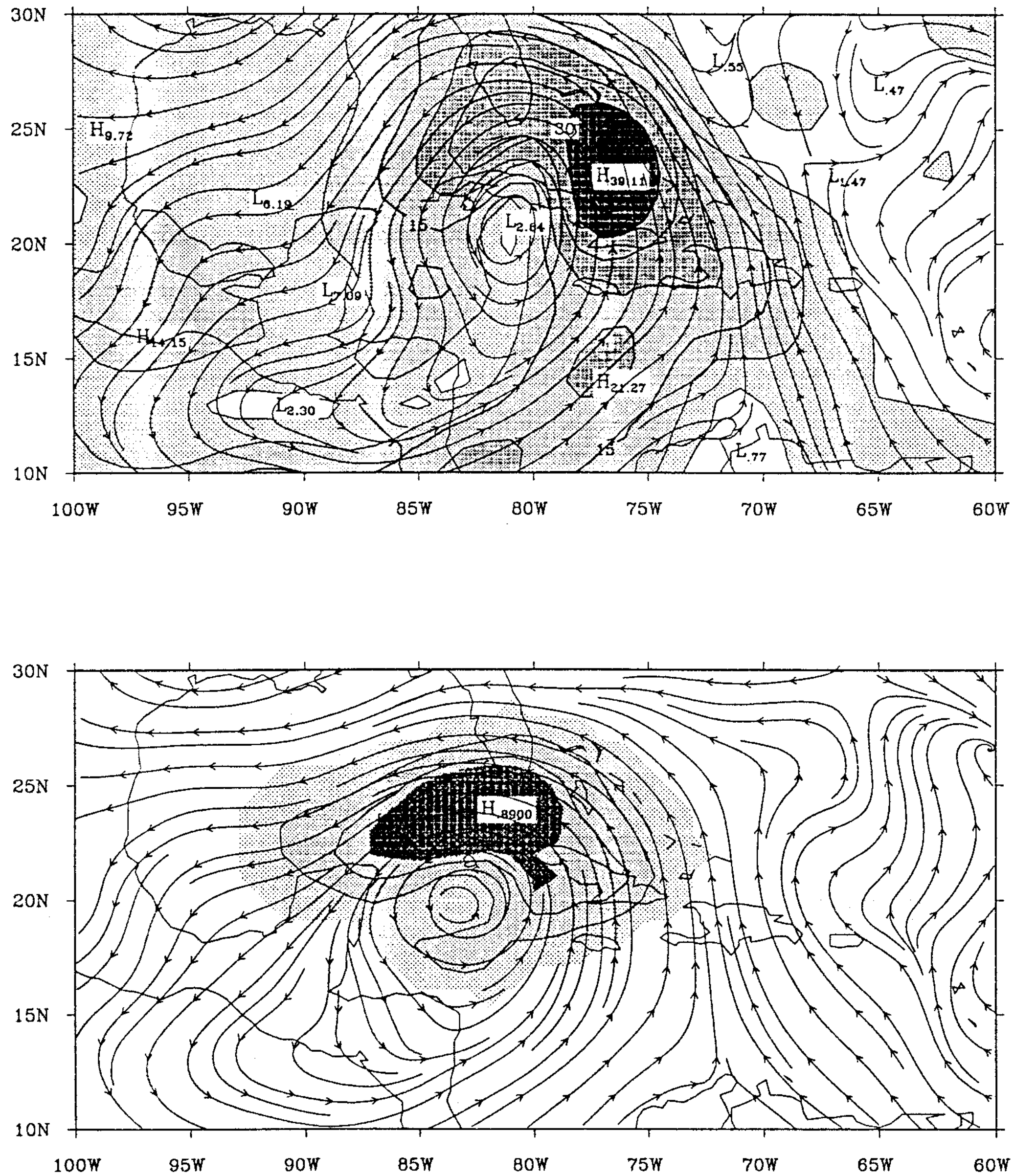

FIG. 8. Hurricane Gilbert: At forecast hour 48, 850-hPa streamlines and isotachs from the (top) control experiment, and (bottom) 850-hPa streamlines from the ensemble mean superimposed by the probability that wind speed is greater than 25 m s^{-1}.

B. The maximum and minimum possible wind speed from individual ensemble members ranged from 25 m s^{-1} to 45 m s^{-1} at location A and 23 m s^{-1} and 55 m s^{-1} at location B. The ensemble wind speed reached its lowest value at forecast hour 36 when the hurricane center was right over the stations. These weakest speeds can also be clearly seen from the outlines of the ensemble maximum and minimum forecasts—that is, the lines linking the maximum points and minimum points. The minimum wind speed predicted by the ensemble members can be as low as 5 m s^{-1} at forecast hour 36 at both locations A and B. However, the control experiment did not predict the hurricane's central weak wind passage. The wind speed decreased slowly after forecast hour 24 in the control experiment. The ensemble wind speed exhibited a secondary peak at hour 48 at both locations A and B. These peaks were due to the strong wind speed areas east of the hurricane center after Gilbert had passed these locations. Again, the control experiment failed to capture this secondary peak at either location. The control curve is very flat after hour 36. For the surface pressure forecast, both the control and the ensemble experiments predicted almost identical pressure values up to hour 24 at both locations A and

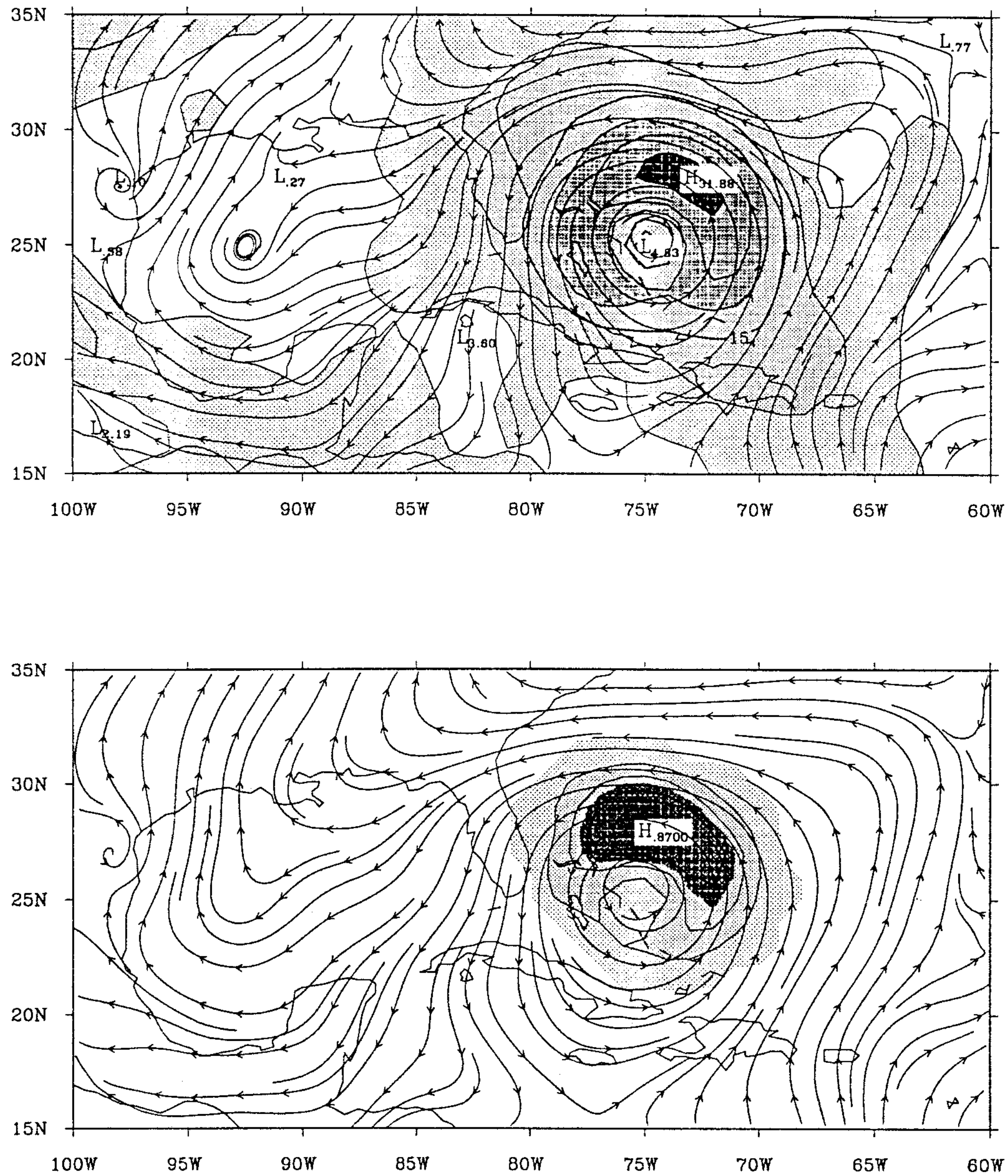

FIG. 9. Same as Fig. 8 but for Hurricane Andrew.

B. The spread of individual ensemble members began at hour 24 and became larger as forecast proceeded. The surface pressures from both experiments reached their lowest point at hour 36 when the hurricane center was right at the stations. It can be seen that the surface pressure predicted by the ensemble experiment is 8-hPa deeper at location A and 4-hPa deeper at location B than that from the control experiment. The minimum surface pressure forecast from one of the ensemble members at hour 36 is about 970 hPa at both locations, compared with the observed surface pressure of 960 hPa. It appears that the ensemble experiment predicted a much stronger hurricane than the control experiment did. The surface pressure and wind speed predicted by the ensemble experiment at locations A and B are closer to the observed values. Therefore, the ensemble prediction greatly improved the intensity forecast in this case.

It should be noted that both the wind speed and the surface pressure plots showed that the dispersion (the length of the vertical bars) becomes larger when the hurricane approaches the location and becomes smaller after the hurricane passes the station. The maximum pressure difference between two individual ensemble members can be as high as 20 hPa at the time when the hurricane is right at the station. The wind speed difference can also be more than 25 m s^{-1}. This feature can be seen for most of the other hurricane cases shown below. This is because the field gradients are so much

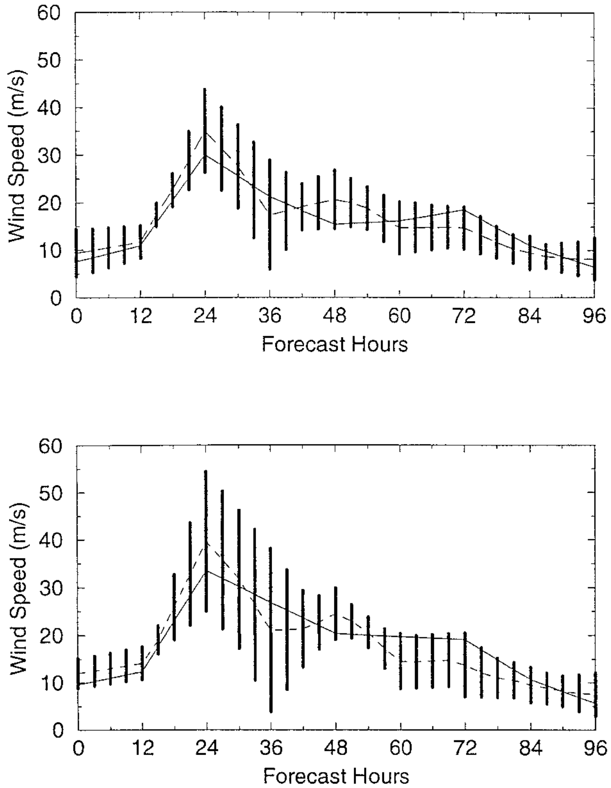

FIG. 10. Hurricane Gilbert: 850-hPa wind speed at two locations on the path of the hurricane. (top) Location A (19.5°N, 78.5°W), (bottom) location B (20.5°N, 82.5°W). The solid line is the control forecast and the dashed line is the ensemble forecast. The vertical bars indicate the possible ranges of wind speed at corresponding forecast time.

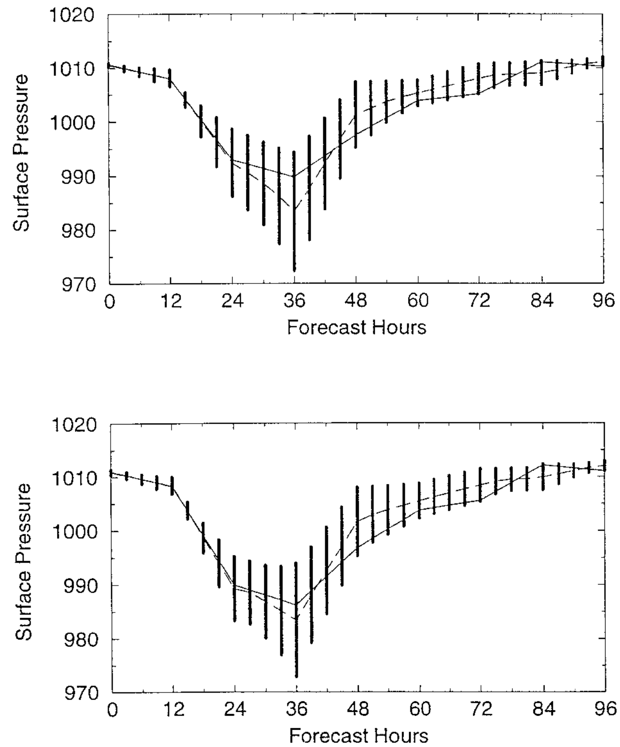

FIG. 11. Hurricane Gilbert: Surface pressure at two locations on the path of the hurricane. (top) Location A (19.5°N, 78.5°W), (bottom) location B (20.5°N, 82.5°W). The solid line is the control forecast and the dashed line is the ensemble forecast. The vertical bars indicate the possible ranges of surface pressure at corresponding forecast time.

stronger near the center of the hurricane, so that any errors of position create large differences. The dispersion of the forecast values from individual ensemble members is actually a measure of the predictability or forecast reliability. The smaller the extreme range, the more reliable is the forecast.

Figure 12 shows the time evolution of surface pressure and wind speed at a fixed location (30°N, 70°W), which is located outside the path of Hurricane Gilbert. The plot has the same coordinate scale as Figs. 10 and 11. It is very clear that these forecast dispersions are much smaller than those at the locations under the influence of the hurricane. The surface pressure spread is around 2 hPa, and the wind speed dispersion is less than 7 m s^{-1}.

e. Ensemble forecast of precipitation and probability distributions

In practical terms, accumulated rainfall is possibly the most important meteorological variable in hurricane prediction. It is also one of the most difficult variables to validate. There are generally two ways to present an ensemble precipitation forecast. One is to show the precipitation forecast from the control experiment together with its two-dimensional probability distribution. The probability can be calculated within the different categories for different purposes. For instance, if rain or no rain in a specific area is of main concern, we can choose to calculate the probability that the model precipitation forecast from different ensemble members is greater than 5 mm in the interested period. If, however, the heavy rainfall area is of main concern, it would be more appropriate to select a category such as the possibility of rain rate greater than 50 mm in a chosen period. The second way to present the ensemble prediction is to show two-dimensional plots of precipitation from each individual ensemble member. The advantage of this method is that it allows us to use our dynamic and synoptic knowledge to find the most plausible rainfall pattern.

Figure 13 is a typical figure presenting ensemble prediction of the accumulated precipitation for the 36–48-h forecast period from the control experiment (Fig. 13 top) and probability of precipitation greater than 25 mm in the 36–48-h period (Fig. 13 bottom) for Hurricane Gilbert. It appears that the control experiment predicted two heavy rainfall centers in the vicinity of the hurricane. One is a west–east-oriented belt with a maximum 31.68 mm and the other is south–north oriented with

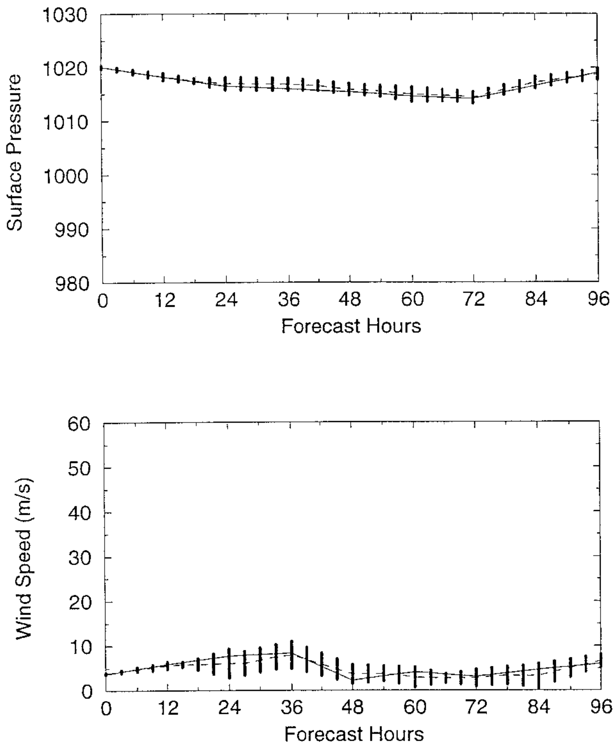

FIG. 12. Hurricane Gilbert: (top) Surface pressure and 850-hPa (bottom) wind speed at a selected location outside of the hurricane (30°N, 70°W). The solid line is the control forecast and the dashed line is the ensemble forecast. The vertical bars indicate the possible ranges of surface pressure and wind speed at corresponding forecast times, respectively.

maximum rainfall of 34.39 mm. However, it is apparent that the probability distribution of precipitation greater than 25 mm does not agree with this two-dimensional rainfall pattern. It has only one center, which is coincident with the west–east oriented precipitation center in the control forecast. The probability suggests that there is an 88% chance that precipitation at this region will exceed 25 mm in 12 h. For the south–north-oriented rainfall center, the ensemble probability shows only a 20%–40% chance that rainfall could exceed 25 mm. This kind of statistical information is very useful in providing guidance to the forecaster on prediction of heavy rainfall areas.

Figure 14 gives an example of precipitation probability for the different categories. Figure 14 (top) is the two-dimensional probability distribution of precipitation greater than 5 mm for the forecast period of hours 36–48. Figure 14 (bottom) shows the probability of rainfall greater than 50 mm in the period between hours 48–60. Both are from the Hurricane Gilbert forecasts. The 5-mm category gives a general idea of where the rainfall would most likely be, whereas the 50-mm category is more focused on the heavy rainfall area of the hurricane. This pattern provides more specific information as to where the heavy rainfall is most likely to be in a statistical sense.

The ensemble mean and the two-dimensional probability distributions can provide only general statistical information. However, sometimes the details of a precipitation forecast from each individual ensemble member may help us to obtain the entire picture of ensemble forecasts. By looking at all of the precipitation forecast patterns from different ensemble members, we will be able to see how sensitive the precipitation forecasts are to the model's initial state.

Figure 15 shows the precipitation forecasts for hours 48–60 from the different ensemble members for Hurricane Gilbert. We will refer to the control experiment and four position perturbed patterns as C (control), N (north), S (south), E (east), and W (west), respectively. The letters P and M indicate plus and minus EOF patterns. For example, CP is the forecast whose initial state is control analysis plus EOF perturbation. Figure 15a is actually the precipitation forecast from the control experiment. The five patterns in the first column—Figs. 15a,d,g,j,m—are the forecasts from the initial states perturbed purely by hurricane position displacement. The forecasts from the initial states perturbed by both hurricane positions and amplitudes are shown in the second and third columns.

For comparison, all of the patterns use the same contour interval of 10 mm. It appears that the location of the maximum rainfall centers are quite different from pattern to pattern, as well as the amount of predicted precipitation. For instance, in pattern C (control experiment), the maximum rainfall center is located at about (22.5°N, 83°W), whereas some of the patterns have two centers associated with hurricane rainfall (e.g., patterns CM and EM) and their centers are located far away from the center of the control experiment. The maximum amount of predicted precipitation for the control run is around 180 mm in 12 h, whereas the forecasts from other members of the ensemble range from 30 mm to 240 mm during the same period. The rainfall distributions from the various ensemble members have different shapes. The precipitation from the control experiment is oriented northwest and southeast, whereas pattern S shows a northeast and southwest orientation. The advantage of showing the forecasts from all of the ensemble members is that we can assimilate these ensemble patterns visually in a subjective manner. By looking at these plots, we may develop our own method to interpret the usefulness of this ensemble spread. For example, in the Gilbert case, we may take out patterns C, NP, and WP because of their lower probabilities, then determine the ensemble precipitation forecast by an average of the remaining members. We can also consider patterns C, NP, and WP as another possibility.

f. Ensemble forecasting variables

Hurricane prediction generally involves two aspects: position prediction and intensity prediction. If we are

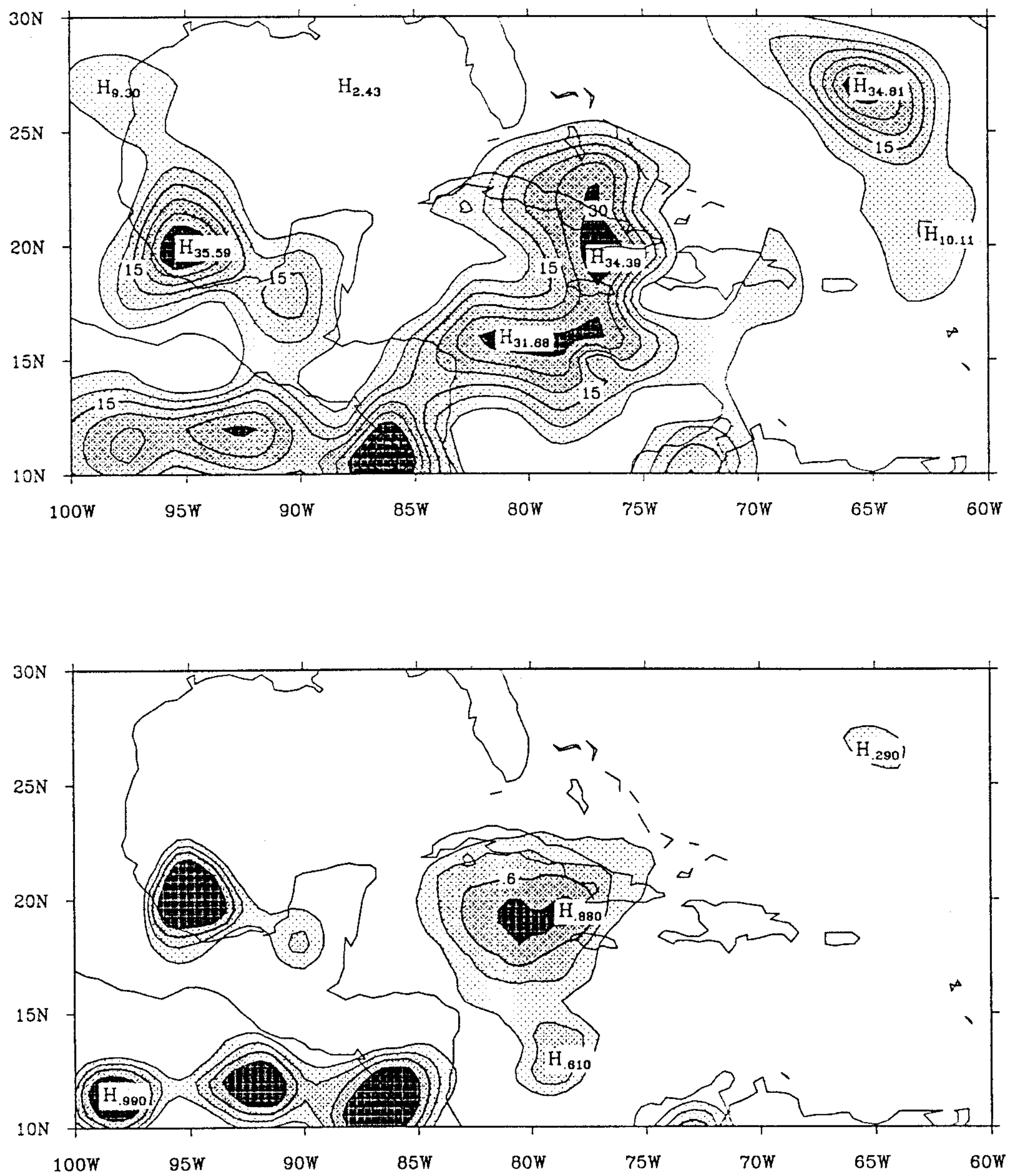

FIG. 13. Hurricane Gilbert: (top) Accumulated precipitation for 36–48 h from control forecast. (bottom) Probability distribution of precipitation greater than 25 mm for 36–48 h (bottom).

interested in intensity prediction, it is not generally recommended to calculate the ensemble mean over the hurricane domain. The reason is that since predicted hurricane positions from various ensemble members are very different, as was shown in the section on track forecasts, an averaging over ensemble members will greatly reduce the hurricane intensity. An alternative method would be to display the results from each of the ensemble members, as we have done for the rainfall distributions. In this section, we will show the ensemble forecasts of surface pressure and geopotential heights at different levels, wind fields at different levels, and the temperature fields. Then we will compare these ensemble results with the control experiment (single model run).

Figure 16 is the surface pressure field for different ensemble members for Hurricane Gilbert. As we can see, the initial perturbations between different ensemble members were very small. It is even difficult to tell the difference by visual inspection. If we look carefully, though, we can find the hurricane positions to be slightly displaced. All of the other initial ensemble fields have the same feature. The corresponding fields for forecasts at day 2 are illustrated in Figs. 17–19. The sea level pressure fields (Fig. 17) are totally different from one ensemble member to the other with respect to hurricane

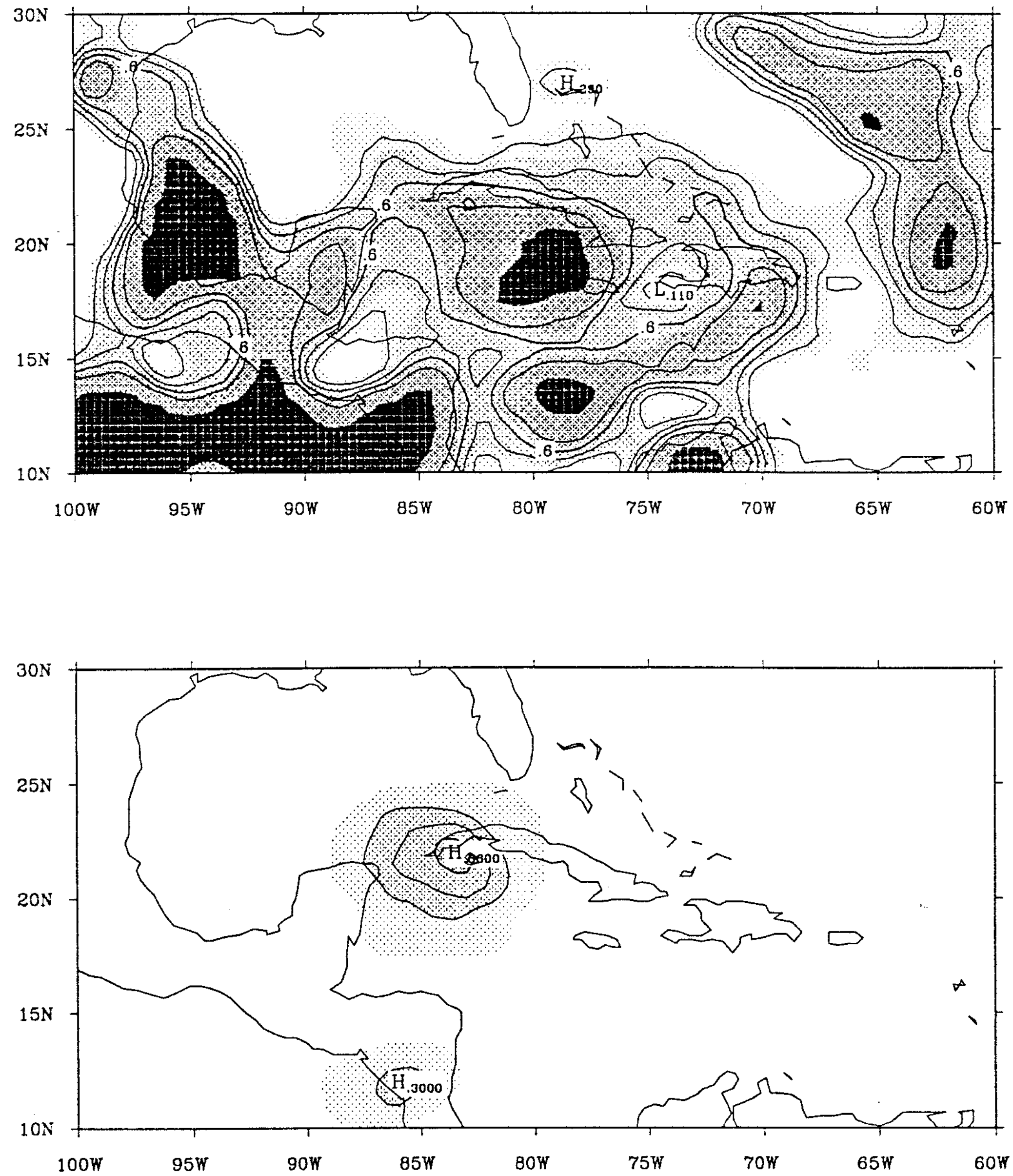

FIG. 14. Hurricane Gilbert: (top) Probability of precipitation greater than 5 mm in the period of 36–48 h; (bottom) probability of precipitation greater than 50 mm in the period of 48–60 h.

shape, size, intensity, and position. In the discussion hereafter, we will use the same convention adopted as in the discussion of the ensemble rainfall distributions. The predicted hurricane positions are scattered throughout a 5° × 5° area. For example, the hurricane position predicted by the control experiment (Fig. 17a) is closer to (22.0°N, 80.5°W), whereas the hurricane in Fig. 17l is located at (20.0°N, 85°W). As we can see, only a few hurricanes are predicted at the north part of the domain (Fig. 17a and Fig. 17g), which is not correct, compared with the observed hurricane position at the same time. Some ensemble members predicted a relatively intense hurricane, for example, Fig. 17k (974 hPa) and Fig. 17n (986 hPa), whereas others predicted a weaker hurricane, for example, Fig. 17d (998 hPa) and Fig. 17i (998 hPa). From the 500-hPa height plot (Fig. 18), we can see more vertical structure within the hurricane from different ensemble members. The predicted hurricane in Fig. 18k remains just as intense at 500 hPa as it is at the surface field, which indicates a vertically consistent structure. On the other hand, although the sea level pressure in Fig. 18l is nearly the same as that of Fig. 18k, Fig. 18l has only one closed contour at 500 hPa, indicating this hurricane has a shallow vertical structure. The difference in 500-hPa heights among the panels is as much as 240 m. The 850-hPa streamlines at forecast day 2 is shown

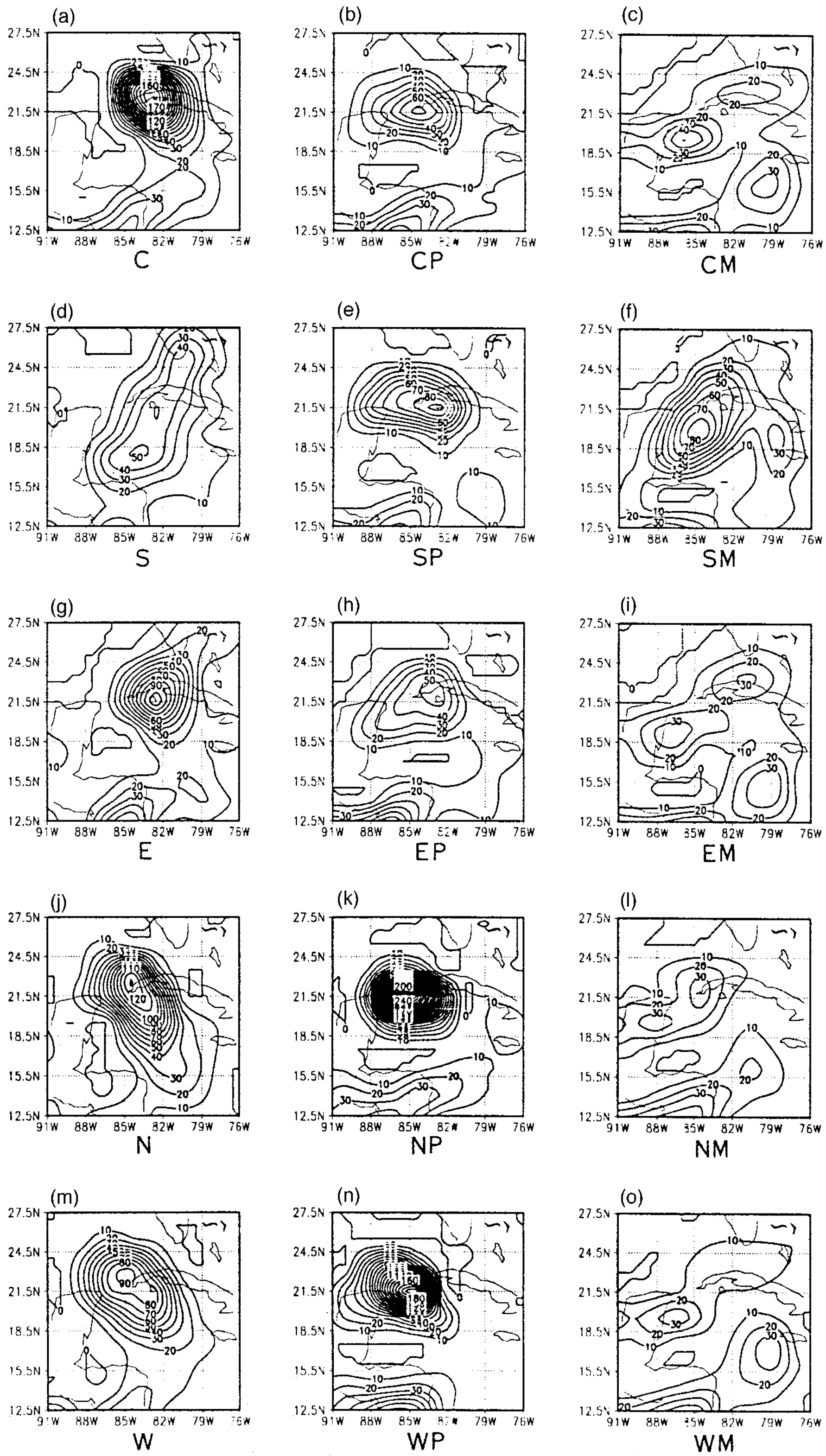

FIG. 15. Hurricane Gilbert: Accumulated precipitation forecast for 48–60 h from individual ensemble members. The pattern in the upper-left corner is from the control experiment. The patterns in the first column are from positional shift samples; the rest are EOF perturbed samples.

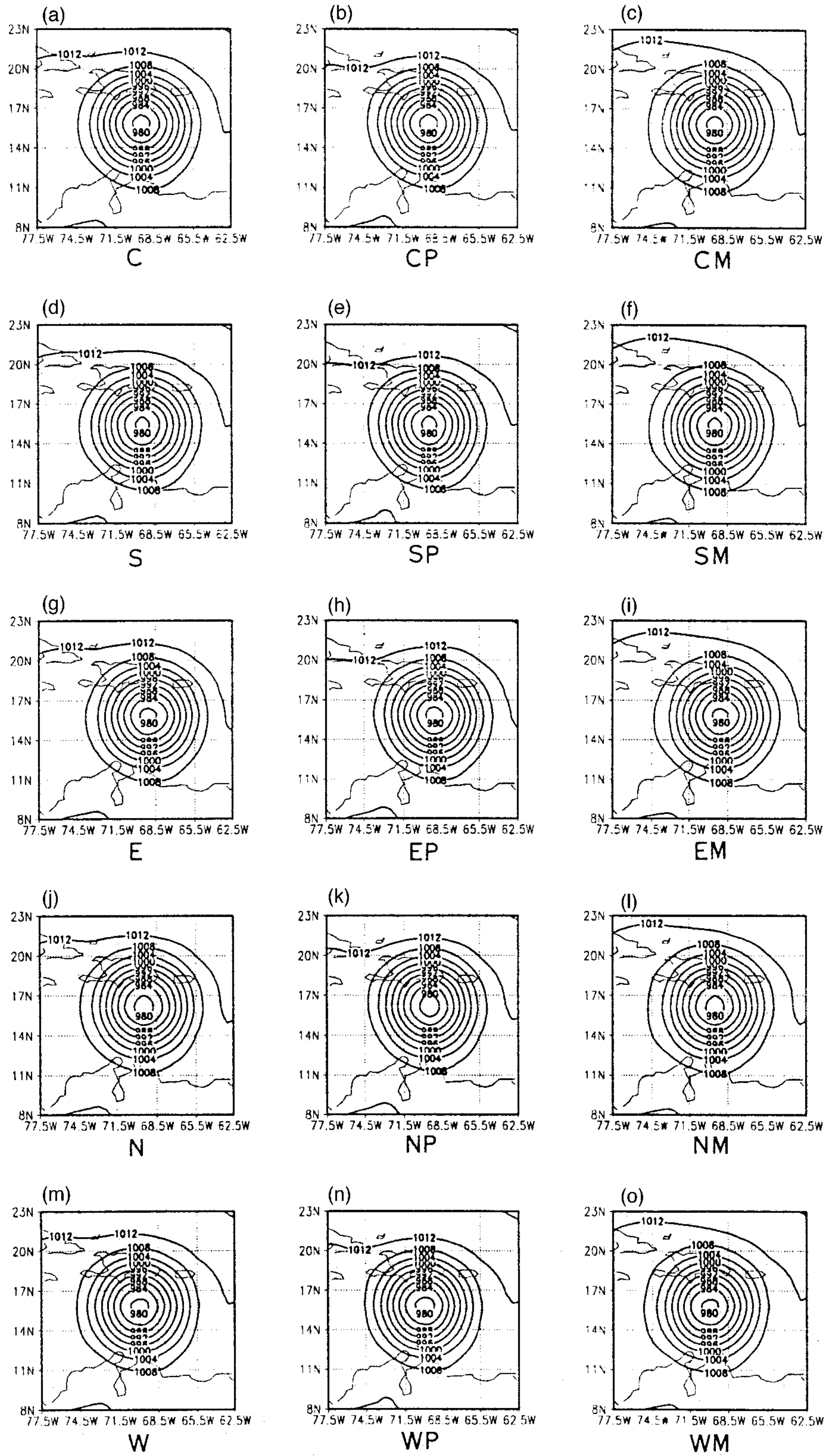

FIG. 16. Hurricane Gilbert: Surface pressure at day 0 from individual ensemble members.

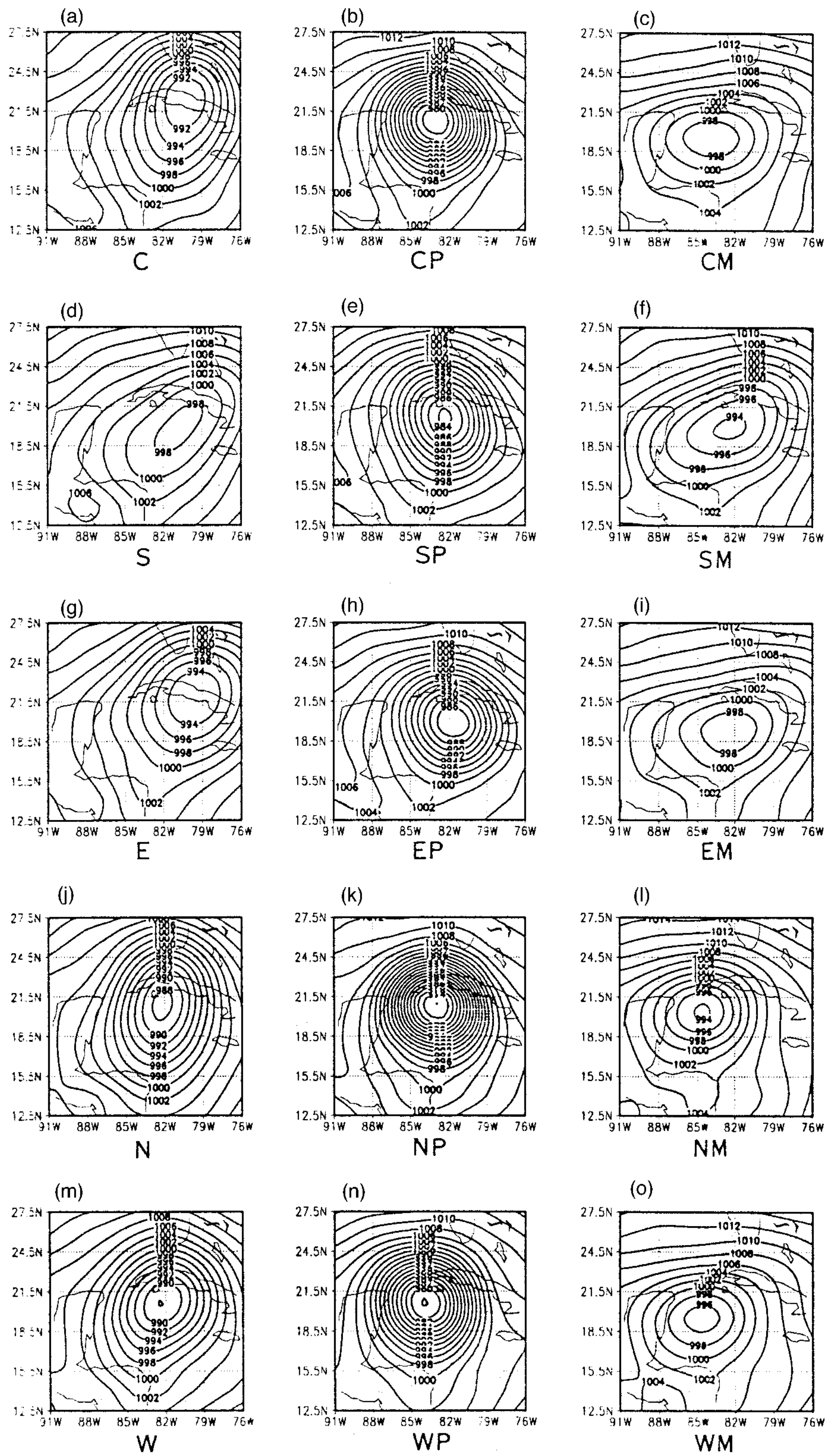

FIG. 17. Hurricane Gilbert: Sea level pressure fields at day 2 from individual ensemble members.

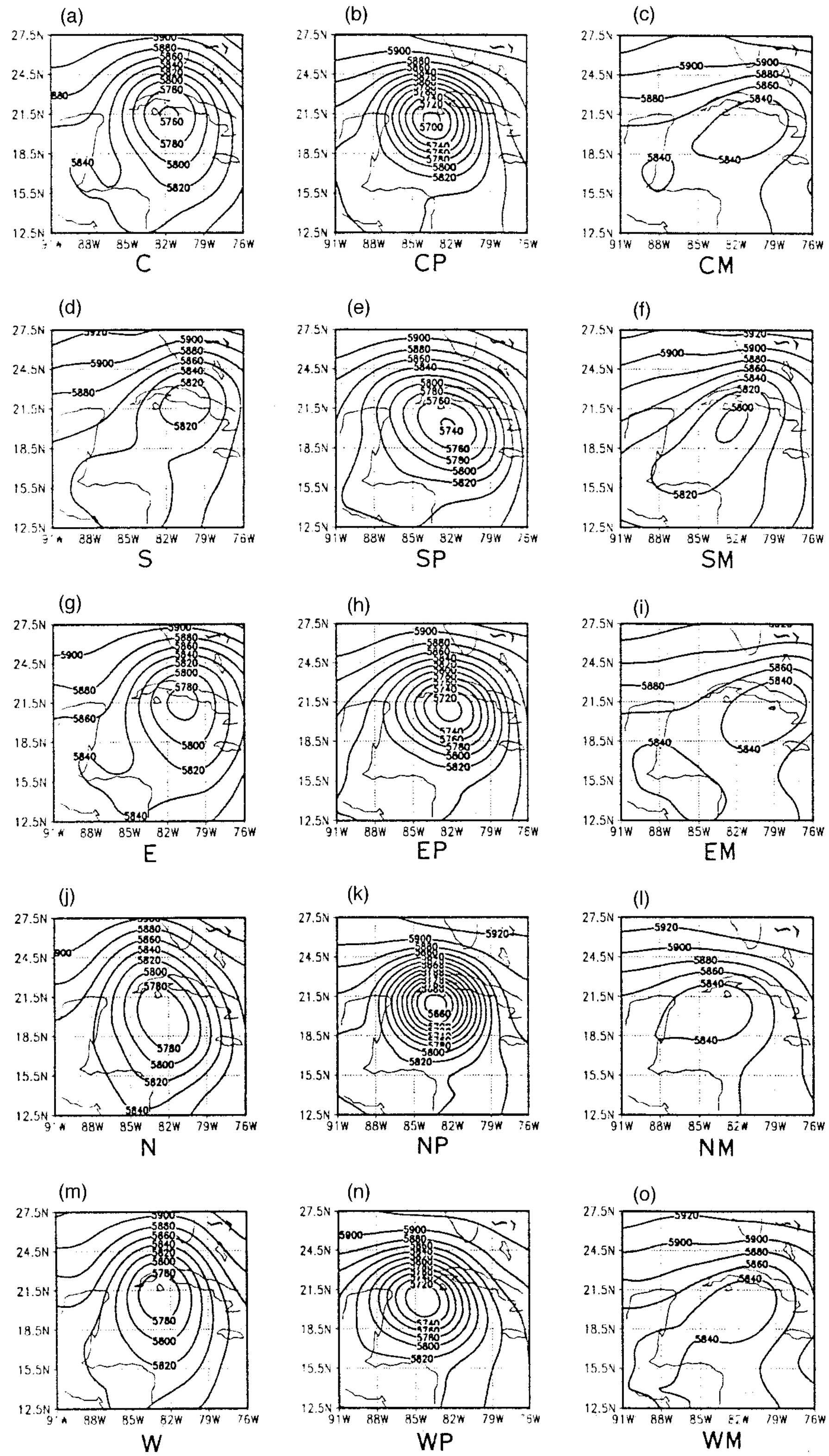

FIG. 18. Hurricane Gilbert: 500-hPa geopotential heights fields at day 2 from individual ensemble members.

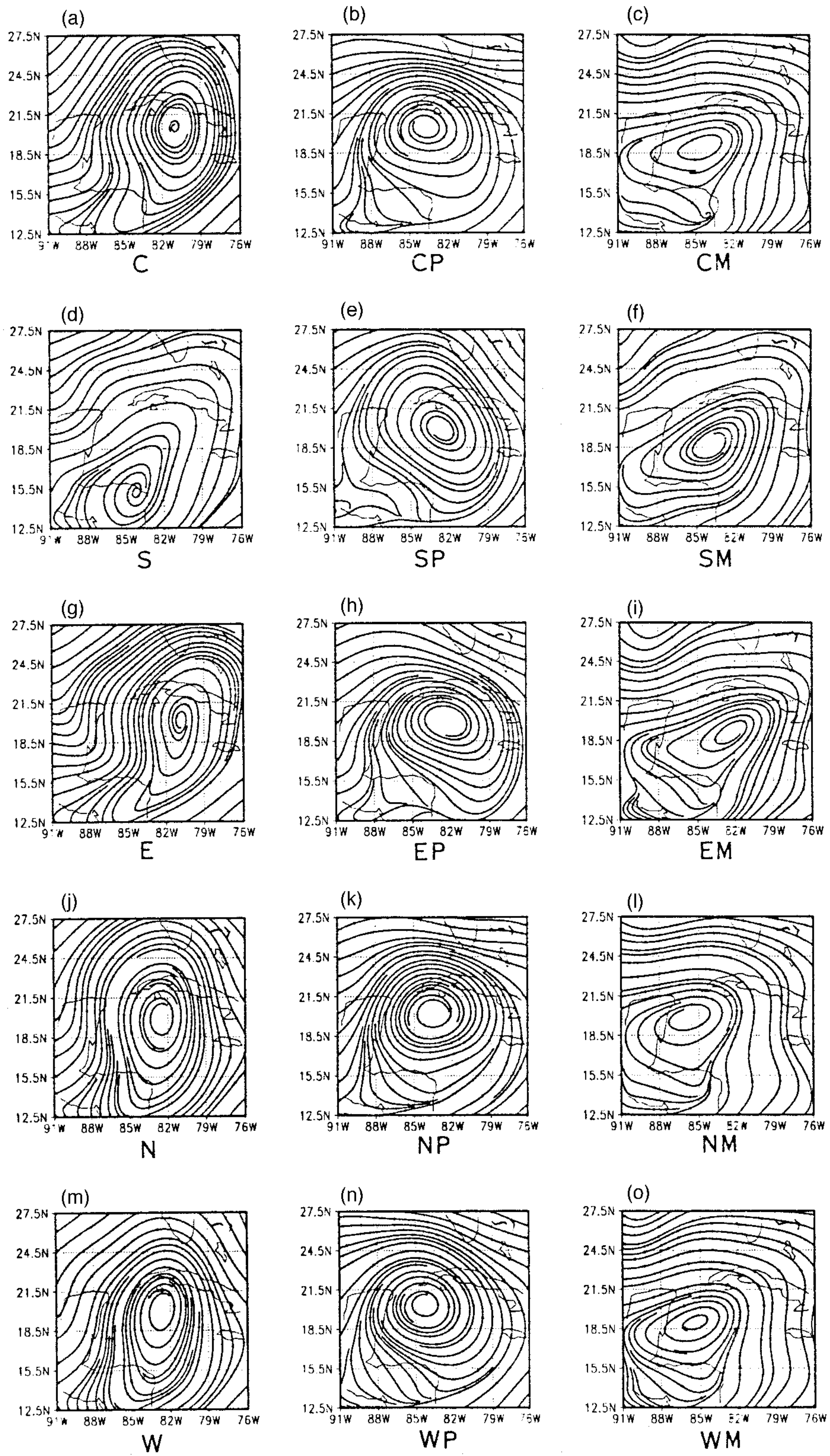

FIG. 19. Hurricane Gilbert: 850-hPa wind fields at day 2 from individual ensemble members.

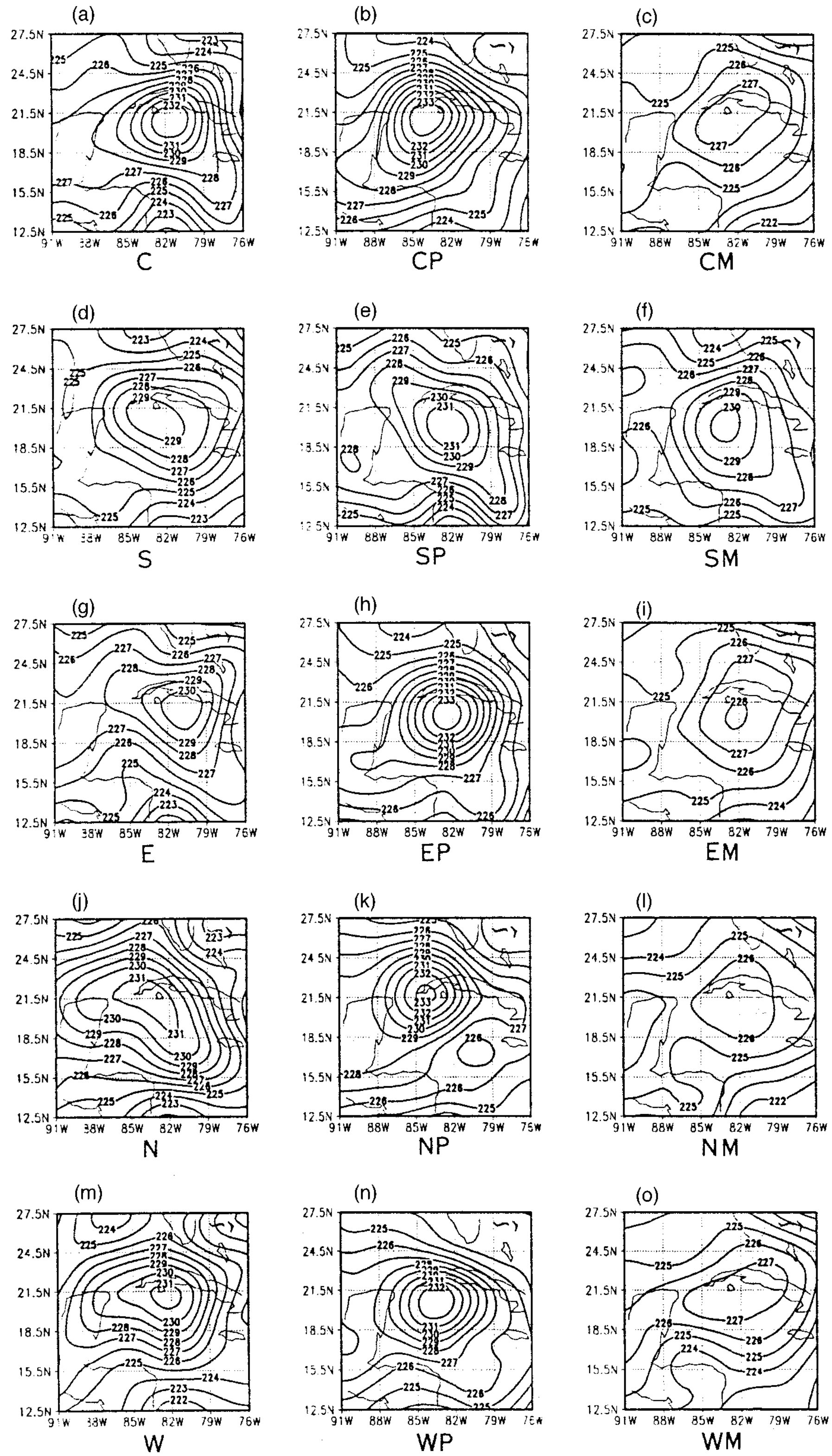

FIG. 20. Hurricane Gilbert: 200-hPa temperature fields at day 2 from individual ensemble members.

in Fig. 19. Although the isotachs are not superimposed due to the smallness of the plots, the spacing among adjacent streamlines provides a measure of the strength of the wind speed.

The 200-hPa ensemble temperature fields at day 2 of the forecast, from individual ensemble members, are shown in Fig. 20 for the Hurricane Gilbert case. As may be seen from Fig. 20, the warm core is well maintained in each panel, although the magnitudes and the central positions are not the same. The temperature gradient across the hurricane in Fig. 20k and Fig. 20b are stronger than that in other panels. It should be noted that although the maximum temperatures in the hurricane center are very different from ensemble member to member, varying from 228 K to 233 K, the environmental temperatures all lie around 224 K.

6. Concluding remarks

The purpose of this study was to apply the ensemble technique to hurricane forecasting and hence to improve the hurricane prediction. Since there is no existing theory to generate perturbations for a hurricane ensemble, an alternative method, EOF-based perturbation method, has been developed and examined in this study. This method includes the large-scale environment perturbations and hurricane position perturbations. The overall hurricane forecast skill is evidently improved by applying this proposed method. The improvements are shown in two statistical aspects: (a) the hurricane track position errors are reduced compared to the control experiment, and (b) the ensemble hurricane structures are reasonably close to typical structures of hurricane observations.

We have shown that EOF-based perturbations grow faster than random perturbations. The experimental results were examined for each hurricane case with respect to both track forecasts and hurricane structures; most of the detailed results are presented for Hurricane Gilbert. An overall improvement in the prediction of this hurricane was noted, as expected. In addition, the following points were observed.

- The statistics include the two-dimensional probability distribution for the maximum wind speed and precipitation. As shown in the results, the centers of maximum hurricane wind speed and precipitation are not always coincident with the centers of maximum probability of wind speed and precipitation. This information allows us to evaluate the control forecast in terms of a two-dimensional field—for example, the greatest probability of maximum precipitation provides a guidance on the location of the heavy rainfall.
- The time evolution of the predicted variables, such as sea level pressure and the wind speed, superimposed on the ensemble variance at a fixed location. This plot provides not only the regular forecast at a fixed location, but also the maximum and minimum possible values of the predicted variable. Local forecasters can combine this information with conventional data, such as historical record, to arrive at an improved guidance. This could be especially beneficial in situations where the hurricane is directly approaching a highly populated region.
- Multipanel charts of the the ensemble members showed the forecast variability within the ensemble. We have shown that the forecasts from individual ensemble members are very different from each other with respect to hurricane dimensions, positions, and intensities. This plot provides an overall picture of ensemble prediction and the reliability of the control forecast. By comparing the subensemble members, it is concluded that both initial hurricane intensity and position perturbations contribute to the spread of the ensemble prediction, therefore, they are equally important to the hurricane ensemble prediction.

Ensemble prediction is a relatively new area of research. This study is a first attempt to apply an ensemble technique for hurricane forecasting with numerical models. Many problems still remain unsolved in this area, such as a reasonable sample size that allows us to extract useful statistical information, the application of ensemble method to higher resolution hurricane models, the reduction of computer time by using parallel computing techniques, etc.

Finally, one should point out that the proposed ensemble prediction method in this study needs to be examined with more hurricane cases before any definitive conclusion can be made. We have recently applied this method with a higher resolution model at FSU to do the real-time forecast of tropical storms in 1997 and the results are very promising. Further research is continuing to explore the behavior of the proposed strategy.

Acknowledgments. This research was supported by NSF Grant ATM-9710336, ONR Grant N00014-95-1-1132, and NASA Grant numbers NAG5-4729 and NAG-81199.

REFERENCES

Buizza, R., 1997: Potential forecast skill of ensemble prediction and spread and skill distributions of the ECMWF ensemble prediction system. *Mon. Wea. Rev.,* **125,** 99–119.

Ebisuzaki, W., and E. Kalnay, 1991: Ensemble experiments with a new lagged analysis forecasting scheme. Research Activities in Atmospheric and Oceanic Modeling. Rep. **15,** WMO, 423 pp. [Available from WMO, C. P. No. 2300, CH1211, Geneva, Switzerland.]

Epstein, E. S., 1969: Stochastic dynamic prediction. *Tellus,* **21,** 739–759.

Hamill, T. M., and S. J. Colucci, 1997: Verification of eta–RSM short-range ensemble forecasts. *Mon. Wea. Rev.,* **125,** 1312–1327.

Hoffman, R. N., and E. Kalnay, 1983: Lagged average forecasting, an alternative to Monte Carlo forecasting. *Tellus,* **35A,** 100–118.

Houtekamer, P. L., and L. Lefaivre, 1997: Using ensemble forecasts for model validation. *Mon. Wea. Rev.,* **125,** 2416–2426.

Krishnamurti, T. N., and H. S. Bedi, 1988: Cumulus parameterization and rainfall rates, Part III. *Mon. Wea. Rev.,* **116,** 583–599.

——, S. Low-Nam, and R. Pasch, 1983: Cumulus parameterization and rainfall rates, Part II. *Mon. Wea. Rev.,* **111,** 815–828.
——, D. Oosterhof, and N. Dignon, 1989: Hurricane prediction with a high resolution global model. *Mon. Wea. Rev.,* **117,** 631–669.
——, C. Ricardo, G. Rohaly, D. Oosterhof, and N. Surgi, 1997: Physical initialization and hurricane ensemble forecasts. *Wea. Forecasting,* **12,** 503–514.
Kurihara, Y., M. A. Bender, and R. J. Ross, 1993: An initialization scheme of hurricane models by vortex specification. *Mon. Wea. Rev.,* **121,** 2030–2045.
Legler, D. M., 1983: Empirical orthogonal function analysis of wind vectors over the tropical Pacific region. *Bull. Amer. Meteor. Soc.,* **64,** 234–241.
Leith, C. E., 1974: Theoretical skill of Monte Carlo forecasts. *Mon. Wea. Rev.,* **102,** 409–418.
Lorenz, E. N., 1963: Deterministic non-periodic flow. *J. Atmos. Sci.,* **20,** 130–141.
——, 1965: A study of the predictability of a 28-variable atmospheric model. *Tellus,* **17,** 321–333.
Molteni, F., R. Buizza, T. N. Palmer, and T. Petroliagis, 1996: The ECMWF ensemble prediction system: Methodology and validation. *Quart. J. Roy. Meteor. Soc.,* **122,** 73–119.
Palmer, T. N., F. Molteni, R. Mureau, R. Buizza, P. Chapelet, and J. Tribbia, 1992: Ensemble prediction. ECMWF Research Department. Tech. Memo. 188, 30 pp. [Available from ECMWF, Shinfield Park, Reading, RG2 9AX, United Kingdom.]
Radford, A. M., J. T. Henning, and J. C. L. Chan, 1995: A new TC bogus scheme at the UK Met Office. Preprints, *21st Conf. on Hurricanes and Tropical Meteorology,* Miami, FL, Amer. Meteor. Soc., 243–245.
Ross, R. J., and Y. Kurihara, 1992: A simplified scheme to simulate asymmetries due to the beta effect in barotropic vortices. *J. Atmos. Sci.,* **49,** 1620–1628.
Toth, Z., and E. Kalnay, 1993: Ensemble forecasting at NMC: The generation of perturbations. *Bull. Amer. Meteor. Soc.,* **74,** 2317–2330.
——, and ——, 1998: Ensemble forecasting at NCEP and the breeding method. *Mon. Wea. Rev.,* **125,** 3297–3319.
Tracton, M. S., and E. Kalnay, 1993: Operational ensemble prediction at the National Meteorological Center. Practical aspects. *Wea. Forecasting,* **8,** 379–398.
Zhang, Z., 1997: Hurricane ensemble prediction using EOF-based perturbations. Ph.D. dissertation, The Florida State University, 174 pp. [Available from Dept. of Meteorology, The Florida State University, Tallahassee, FL 32306.]
——, and T. N. Krishnamurti, 1997: Ensemble forecasting of hurricane tracks. *Bull. Amer. Meteor. Soc.,* **78,** 2785–2795.